DOI: 10.1002/cbic.200800313

DNA with Branched Internal Side Chains: Synthesis of 5-Tripropargylamine-dU and Conjugation by an Azide-Alkyne Double Click Reaction

Venkata Ramana Sirivolu, Padmaja Chittepu, and Frank Seela*[a]

*5-Tripropargylamine-2′-deoxyuridine (**1a**) containing two terminal triple bonds was synthesized by a Pd-assisted Sonogashira cross-coupling reaction and was subsequently converted into the corresponding phosphoramidite building block (**9**) and employed in solid-phase oligonucleotide synthesis. T_m experiments demonstrate that the presence of covalently attached branched tripropargylamine residues has a positive effect on the base pair stability. The two terminal C≡C bonds of modified DNA were functionalized by means of Cu^I-mediated 1,3-dipolar cycloaddition reactions (click chemistry) with azides such as 3-azido-7-hydroxycoumarin or 3′-azido-3′-deoxythymidine (AZT) both in solution and on solid support. In particular, with the nonfluorescent 3-azido-7-hydroxycoumarin a strongly fluorescent oligonucleotide bis-dye conjugate was generated. For comparison, the N(3)-propargylated 2′-deoxyuridine **2** was prepared from 2′-deoxyuridine and propargyl bromide and incorporated into DNA. The two terminal triple bonds of **1a** allow the simultaneous post-modification of DNA by two reporter molecules and can be applied to almost any azido derivatives (oligonucleotides, proteins, polysaccharides etc.) including those forming dendrimeric side chains.*

Introduction

The Cu^I-catalysed Huisgen–Sharpless–Meldal cycloaddition,[1–5] click chemistry, has become a key reaction for introducing reporter groups into carbohydrates,[6] proteins[7,8] and nucleic acids.[9–14] This reaction has been performed with DNA in solution, on solid support[15] and on surfaces[16] including biochip devices.[17] Recently, we reported on octa-1,7-diynyl side chain derivatives containing terminal triple bonds[15,18] for fluorescent dye conjugation by the click reaction. Fluorescent dye conjugates of all four DNA building blocks were prepared.[19,20] The side chains were located in the 7-positions of 7-deazapurines or the 5-positions of pyrimidines. This guarantees that bulky dye residues protrude into the major groove of B-DNA.

We now report on the synthesis and properties of oligonucleotides bearing tripropargylamine residues. For this modification we have chosen the 5-position of 2′-deoxyuridine, giving **1a**. A branched element capable of functionalization by two molecular reporter units is thus introduced into a nucleoside. Branched oligonucleotides have already been used as signal amplifiers in nucleic acid quantification for the detection of viral infections,[21] for the construction of i-motif structures[22] and for various other purposes.[23–26] Polylabelled DNA probes[27] have also been employed to amplify fluorescence signals in hybridization studies.[28] Here we compare the physical data for compound **1a**, containing two terminal triple bonds, with those for the monofunctionalized derivatives **1b** and **2**. While compounds **1a** and **1b** can form Watson–Crick base pairs with dA, the recognition site of **2** is blocked by a short linker. Normally, such functionalization is unfavourable because base pairing is hindered. However, when such a short, stiff linker is introduced the fluorescence can be increased.

Nucleosides **1a** and **2** were converted into phosphoramidite building blocks, and oligonucleotides incorporating these

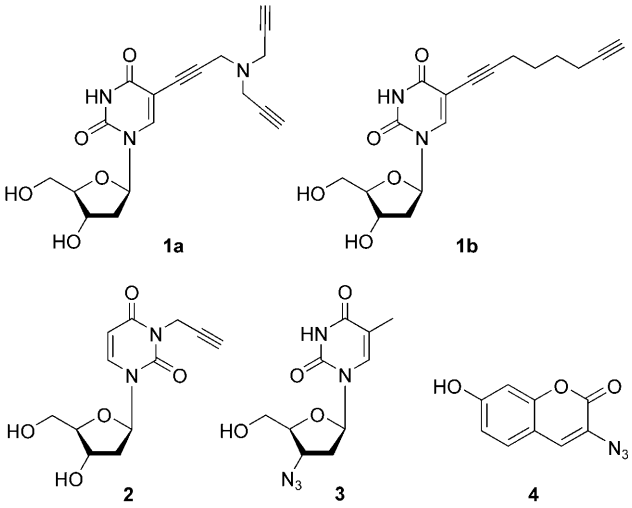

modified units were prepared by solid-phase synthesis. While the linker of **1a** has a length similar to that of the already described **1b**, the linker of **2** is significantly shorter. As compounds **1a**, **1b** and **2** contain terminal triple bonds they can

[a] *V. R. Sirivolu, P. Chittepu, Prof. Dr. F. Seela*
Laboratory for Bioorganic Chemistry and Chemical Biology
Center for Nanotechnology
Heisenbergstrasse 11, 48149 Münster (Germany)
and Laboratorium für Organische und Bioorganische Chemie
Universität Osnabrück
Barbarastrasse 7, 49069 Osnabrück (Germany)
Fax: (+49) 251-53406857
E-mail: frank.seela@uni-osnabrueck.de

Supporting information for this article is available on the WWW under http://www.chembiochem.org or from the author.

be derivatized by Cu^{I}-catalysed azide–alkyne Huisgen–Sharpless–Meldal cycloadditions. For this purpose, either a fluorescent dye reporter or the antiviral active nucleoside AZT (**3**) were chosen (Scheme 1). The click reactions were performed both in solution and on solid support. Both protocols result in the difunctionalization of the side chain in a chemoselective manner.

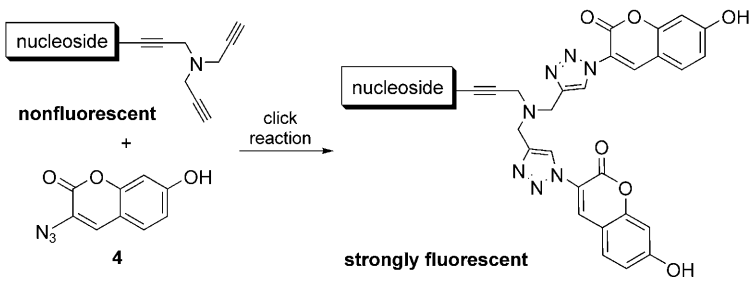

Scheme 1. Cu^{I}-catalysed difunctionalization through alkyne–azide cycloaddition.

Results and Discussion

Synthesis and properties of monomers

The nucleoside **1a** was synthesized from 2′-deoxy-5-iodouridine (**5**) and tripropargylamine by means of the Pd-assisted Sonogashira cross-coupling reaction (Scheme 2). A 1:2 ratio of $Pd(PPh_3)_4$ and CuI and an excess of tripropargylamine were used.[29] Only one terminal triple bond reacts, in chemoselective fashion, in this reaction, leading to the formation of the monofunctionalized nucleoside **1a** in 69% yield. The Pd-cross-coupling reaction of **1a** results in the formation of a trace amount of the fluorescent by-product **6**. Exclusive formation of **6** was achieved when **1a** was cyclized in the presence of CuI.[30]

Treatment of 2′-deoxyuridine (**7**) with propargyl bromide in the presence of K_2CO_3 in DMF afforded 3-propargyl-2′-deoxyuridine (**2**) in 72% yield (Scheme 2).

The introduction of alkynyl substituents at the 5-position of the 2′-deoxyuridine moiety strongly influences the physical properties—such as the pK_a values—of the nucleoside.[15] When we examined the pK_a data for **1a**, two pK_a values were found: one for the base deprotonation (8.3) and the other for the side chain protonation (3.3). As 2′-deoxyuridine shows a pK_a value of 9.3, the side chain of **1a** decrease the pK_a value of the N(3)–H component by one unit, which should strengthen the base pair (better H-donor).[31] On the other hand, the tripropargylamine moiety has a pK_a value of 3.09[32] (for protonation), which is several units lower than that of propargylamine ($pK_a = 8.15$),[33] so the side chain is not protonated under neutral conditions.

Next, building blocks based on **1a** and **2** were synthesized. The 5-tripropargylamine-2′-deoxyuridine (**1a**) was converted into the phosphoramidite **9** via the DMTr derivative **8**. In a similar way, the N(3)-propargylated 2′-deoxyuridine **2** was converted into the dimethoxytrityl derivative **10** and further transformed into the phosphoramidite **11** (Scheme 3). All of the synthesized compounds were characterized by their elemental analyses or mass spectra, as well as by their ^1H and ^{13}C NMR spectra. The ^{13}C NMR chemical shifts are summarized in Table 1. The presence of a tripropargylamine substituent at the 5-position of pyrimidine changes the C(5) chemical shifts of compound **1a** and their derivatives consistently with the electron-withdrawing character of the tripropargylamine residue. From the ^1H NMR spectrum of **1a** the two signals observed at 3.23 ppm (2 C≡CH) and 3.40 ppm (2 C≡C–CH_2) confirmed the intact structure of the side chain. Similar signals were also observed for the furano bicyclic nucleoside **6**. The two acetylene carbons were clearly distinguished by ^{13}C NMR as well as by use of gated-decoupled spectra. The terminal C≡C atoms of the side chains of **1a** and **6** showed C,H coupling ($^1J_{C,H} = 249$–250 Hz).

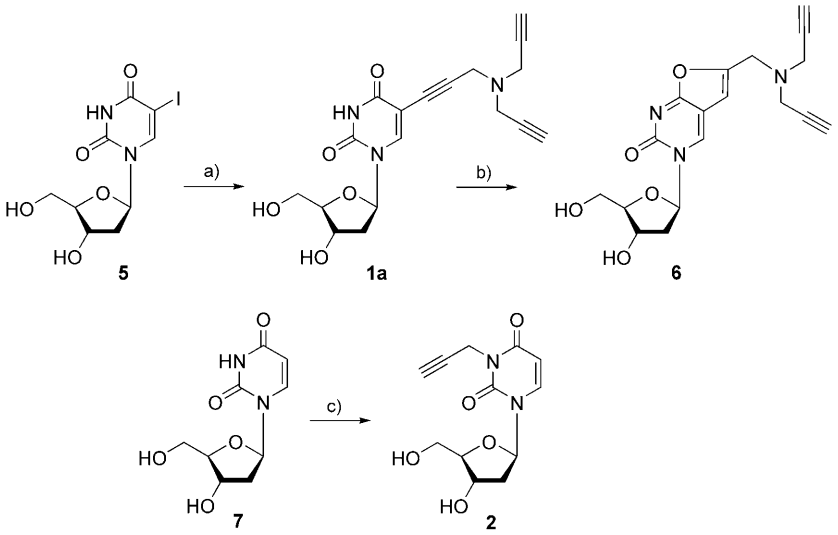

Scheme 2. Synthesis of the alkynyl nucleosides. a) $[Pd(PPh_3)_4]$, CuI, Et_3N, DMF, tripropargylamine; b) CuI, Et_3N/MeOH, 80 °C; c) propargyl bromide, K_2CO_3, DMF.

Oligonucleotides

Synthesis, characterization and duplex stability: Oligonucleotides were prepared by solid-phase synthesis with the phosphoramidites **9** and **11** together with standard building blocks. The coupling yields were always higher than 95%. Deprotection of the oligomers was performed in aqueous NH_3 (25%) at 60 °C over 14 h. The oligonucleotides were detritylated and purified by reversed-phase HPLC. The homogeneities of the oligonucleotides were confirmed by reversed-

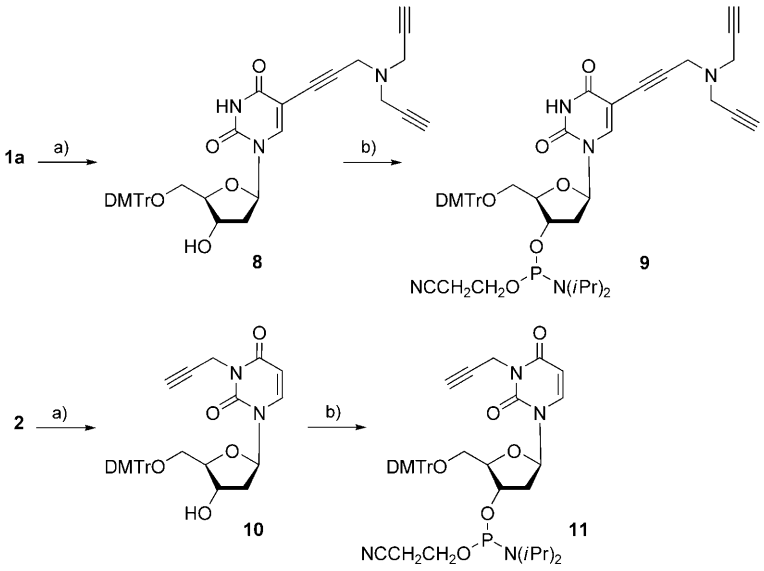

Scheme 3. Synthesis of the phosphoramidite building blocks. a) 4,4′-Dimethoxytriphenylmethyl chloride, anhydrous pyridine, RT, 6 h; b) 2-cyanoethyl-*N*,*N*-diisopropylchlorophosphoramidite, *N*,*N*-diisopropylethylamine, CH_2Cl_2, RT, 1 h.

phase HPLC, as well as by MALDI-TOF mass spectrometry (see Table S1 in the Supporting Information). The base compositions of the oligonucleotides containing **1a** were determined by enzymatic hydrolysis with snake venom phosphodiesterase followed by alkaline phosphatase and subsequent reversed-phase HPLC chromatography (Figure 1).

Our laboratory has reported on the influences on duplex stability of various 5-substituents of pyrimidines and 7-substituents of 7-deazapurines such as halogens and alkynes.[34–37] Of these, propynyl groups are more stabilizing than alkyl groups and the halogeno substituents.[38–41]

We have recently demonstrated that long-chain diynyl linkers such as octadiynyl residues or propargyl ether moieties show a positive influence on duplex stability similar to that brought about by a propynyl residue.[15] The advantage of such linkers is the presence of triple bonds that enhance the hydrophilic character of the linker. The triple bonds can act as electron donors and they can form hydrogen bonds with water molecules. These results prompted us to evaluate the effect of the sterically demanding tripropargylamine group on the duplex stability of DNA. For that purpose, the nucleoside **1a** was incorporated into the reference oligonucleotides 5′-d(TAG GTC AAT ACT)-3′ (**12**) and 3′-d(ATC CAG TTA TGA)-5′ (**13**) by replacing certain dT residues with the modified nucleoside **1a**. Single or multiple incorporation of **1a** resulted in small T_m increases (Table 2). The space-demanding side chain is thus well accommodated in the major groove of the DNA duplex.

In a second series of experiments the oligonucleotide duplex stability was studied with the N(3)-propargylated nucleoside **2** replacing dT at exactly the same positions. As would be expected, duplexes were destabilized because the H-bonding of **2** with dA was blocked by the propargyl residue. However, as described later, this can have a positive influence on the fluorescence. With regard to base-pair stability, these results clearly demonstrate that the 5-tripro-

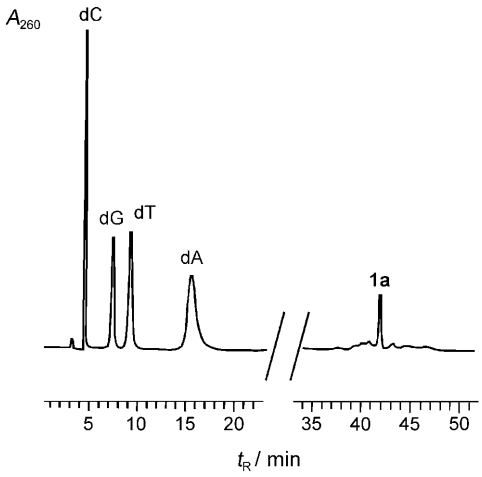

Figure 1. HPLC profile of the enzymatic hydrolysis products of the oligonucleotide 5′-d(TAG G**1a**C AAT ACT) obtained by digestion with snake venom phosphodiesterase and alkaline phosphatase in Tris-HCl buffer (pH 8.5, 0.1 M) at 37 °C. Gradient: 20 min 100% A, 20–60 min 0–30% B in A, flow rate 0.7 mL min^{-1} (A = (Et_3NH)OAc (pH 7.0, 0.1 M)/MeCN 95:5, B = MeCN).

Table 1. ^{13}C NMR chemical shifts (δ) of pyrimidine 2′-deoxyribonucleosides and their derivatives.[a]

Compd	C(2)[b]	C(4)[b]	C(4a)[b]	C(5)[b]	C(6)[b]	C(7a)[b]	C(1′)	C(2′)	C(3′)	C(4′)	C(5′)	triazole	C≡C	CH_2
1a	149.5	161.7		98.0	143.6		84.8	[d]	70.1	87.6[c]	60.9		87.5[c], 79.0 77.4, 76.1	42.8, 41.9
2	149.9	161.0		101.0	139.6		85.4	[d]	70.3	87.6	61.1		78.6, 73.0	29.7
6	153.5	138.4	106.1	104.1	154.1	171.5	87.8	[d]	70.0	88.3	61.0		78.9, 76.4	49.1, 41.5
8	149.4	161.7		98.3	143.0		85.1	[d]	70.4	87.9	63.8		86.0, 78.9 76.9, 76.0	42.1, 41.1
10	149.7	161.0		100.6	139.4		85.2 [c]	[d]	70.0	85.9[c]	63.3		78.6, 72.9	29.7
19	150.6	161.9		101.2	139.6		85.5	[d]	70.4	87.7	61.3	142.9 124.6		35.8
21	149.5	161.8		98.3	143.5		84.8	[d]	70.1	87.6[c]	60.9	143.8 124.9	87.7[c], 77.9	47.3, 42.2

[a] Measured in [D_6]DMSO. [b] Systematic numbering. [c] Tentative. [d] Superimposed by DMSO.

pargylamine nucleoside **1a** shows pairing behaviour very similar to that of dT, with a tendency towards duplex stabilization.

Mono- and difunctionalization of alkynylated nucleosides with 3-azido-7-hydroxycoumarin and their photophysical properties: Cu^{I}-catalysed Huisgen–Sharpless–Meldal cycloadditions were used for the attachment of dyes to the nucleobases. The N(3)-1,2,3-triazolyl coumarin nucleoside **19** was synthesized from the N(3)-propargylated 2′-deoxyuridine **2** and 3-azido-7-hydroxycoumarin (**4**) in the presence of $CuSO_4$ and sodium ascorbate in a 3:1:1 mixture of THF/*t*BuOH/H_2O (80% yield). The two terminal triple bonds of **1a** were then conjugated with the nonfluorescent compound **4**, leading to the formation of a difunctionalized click adduct **21** in 60% yield (Scheme 4). The reaction was performed in acetonitrile by the protocol of Sharpless and co-workers.[42] In this reaction a 2.5-fold excess of the coumarin azide was used to complete a double click conjugation.

The effect of one dye modification versus two dye modifications was studied by use of azidocoumarin as fluorescent reporter group. As one-dye compounds, we chose **19**, with the rigid 1,2,3-triazolyl linked coumarin attached to the N(3)-position of 2′-dU, and also the flexible long-chain 1,2,3-triazolyl-linked coumarin conjugate **20** and compared their fluorescence properties with those of the two-dye-labelled bis-1,2,3-triazolyl coumarin conjugate **21**. The structures of the dye conjugates were confirmed by NMR spectroscopy and mass spectrometry. ^{1}H NMR spectra of **21** revealed the disappearance of two terminal C≡C hydrogens (singlet at 3.23 ppm), whereas the two new singlets appearing around $\delta = 8$–9 ppm are attributed to the protons of the newly formed triazole rings. The signal intensities of the proton signals of two triazole rings clearly demonstrate the formation of the bis-dye adduct. The characteristic signals of the olefinic carbon atoms of the newly formed 1,2,3-triazole moiety were identified at δ(C) = 124.9 and 143.7 ppm (quaternary; Table 1). Moreover, the structure of the triazole ring carbons is clearly attested to by ^{1}H, ^{13}C and 135-DEPT NMR spectra displaying no signal for a quaternary carbon (δ_{C4}) with an inverted signal of the triazole carbon (δ_{C5}) at around 124.9 ppm.

Table 2. T_m values of oligonucleotide duplexes containing modified nucleosides **1a**, **1b** or **2**.[a]

Duplex	T_m [°C]	Duplex	T_m [°C]
5′-d(TAG GTC AAT ACT) (**12**)	50	5′-d(TAG G**1b**C AAT ACT) (**16**)	52
3′-d(ATC CAG TTA TGA) (**13**)		3′-d(ATC CAG TTA TGA) (**13**)	
5′-d(TAG G**1a**C AAT ACT) (**14**)	51	5′-d(TAG GTC AAT ACT) (**12**)	53
3′-d(ATC CAG TTA TGA) (**13**)		3′-d(ATC CAG **1b1b**A TGA) (**17**)	
5′-d(TAG GTC AAT ACT) (**12**)	52	5′-d(TAG G**1b**C AAT ACT) (**16**)	55
3′-d(ATC CAG **1a1a**A TGA) (**15**)		3′-d(ATC CAG **1b1b**A TGA) (**17**)	
5′-d(TAG G**1a**C AAT ACT) (**14**)	53	5′-d(TAG G**2**C AAT ACT) (**18**)	31
3′-d(ATC CAG **1a1a**A TGA) (**15**)		3′-d(ATC CAG TTA TGA) (**13**)	

[a] Measured at 260 nm in NaCl (1 M), $MgCl_2$ (100 mM) and Na cacodylate (pH 7.0, 60 mM) with 5 μM+5 μM single-strand concentration.

The influence of the various side chains on HPLC mobility was determined by injection of an artificial mixture of click products onto the HPLC column. From the HPLC profile shown in Figure 2 the tripropargylamine nucleoside dye conjugate **21** shows a mobility similar to that of the octadiynyl derivative **20**, while the N(3)-alkylated adduct **19** migrates significantly more quickly than **20** and **21**. The number of side chain methylene units of **20** and **21** enhance the hydrophobic character relative to **19**.

Coumarin dyes have been extensively studied because of their favourable photophysical properties. They are used as fluorescent probes to investigate the structural dynamics of DNA, for the specific labelling of nucleic acids and mainly as nucleobase specific quenchers.[43,44] Moreover, it is well known that the fluorescence properties of the coumarin derivative **4** strongly depend on the pH value and the solvent polarity.

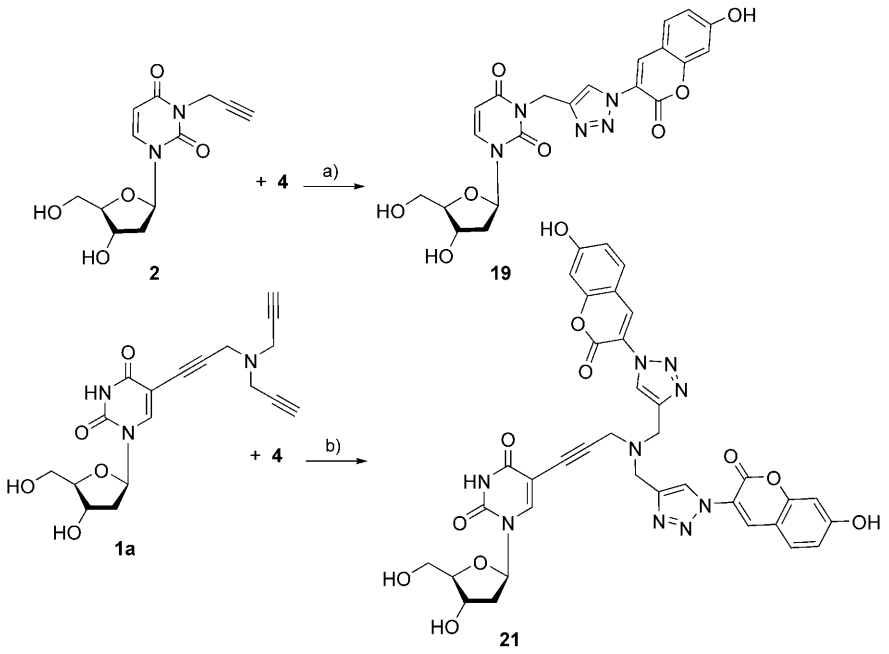

Scheme 4. Synthesis of 1,2,3-triazolyl nucleoside–coumarin conjugates. a) $CuSO_4$, Na ascorbate, THF/*t*BuOH/H_2O, 18 h, RT; b) acetonitrile, 2,6-lutidine, $Cu(MeCN)_4PF_6$, 20 h, RT

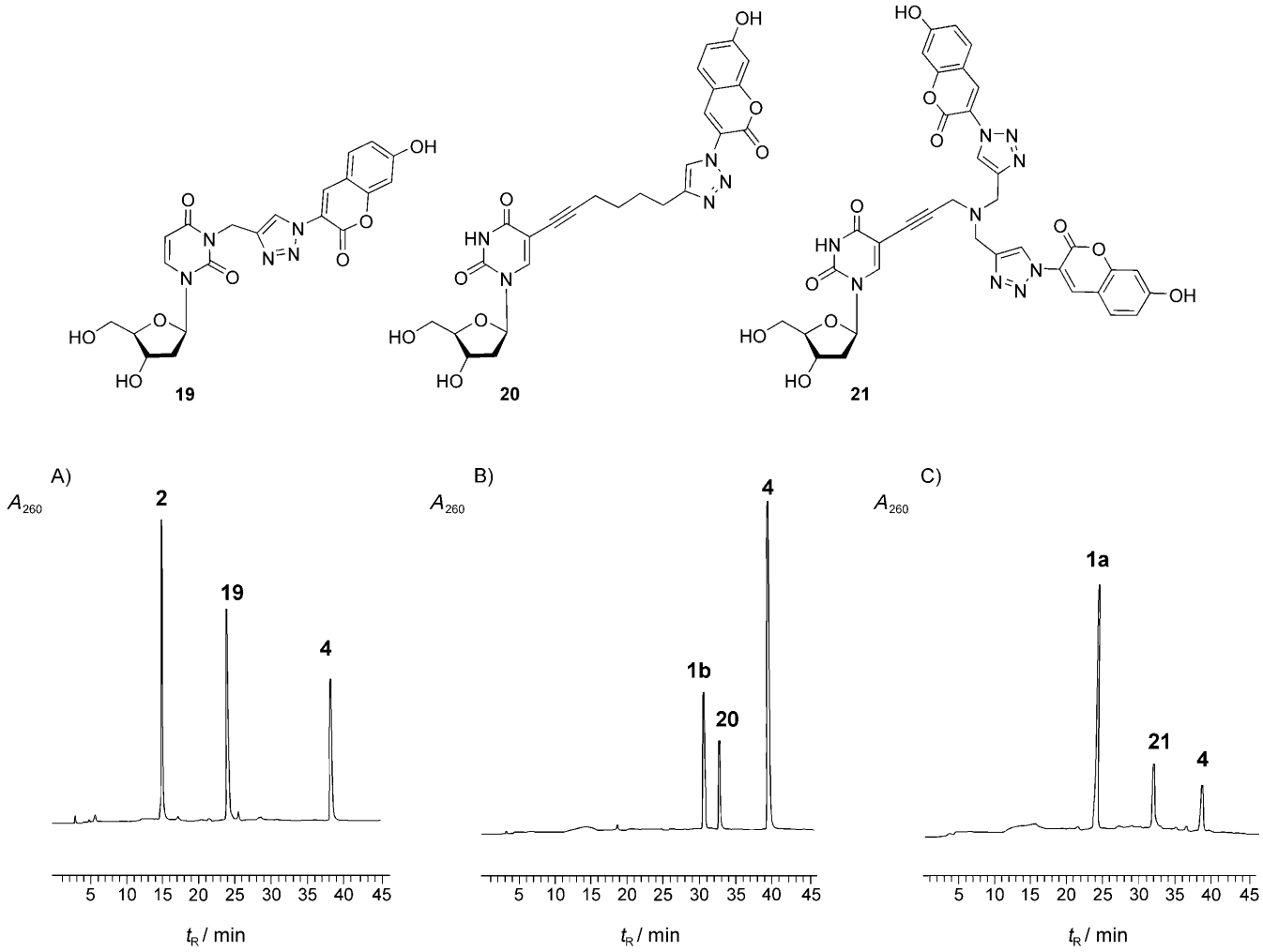

Figure 2. HPLC profiles of a) an artificial mixture of starting compounds **2**, **4** and the click product **19**, b) **1b**, **4** and the click product **20**, and c) **1a**, **4** and the click product **21** on a RP-18 (200×10 mm) column. The following solvent systems were used: A) MeCN, and B) (Et_3NH)OAc (pH 7.0, 0.1 M)/MeCN 95:5. Gradient 0–50 min 0–50% A in B.

Different excitation maxima are found at different pH values, due to the formation of a phenolate anion under alkaline conditions.[45] Whereas 3-azido-7-hydroxycoumarin is not fluorescent, the 1,2,3-triazole coumarin conjugate obtained from the terminal alkynes and 3-azido-7-hydroxycoumarin is strongly fluorescent.[46]

The UV–visible absorption spectra of the nucleoside conjugates **19**–**21**, as well as their fluorescence spectra, were measured in Tris-HCl buffer (pH 8.5) under identical conditions (same solutions for UV and fluorescence measurements; Figure 3). It is apparent that in the case of nucleoside-coumarin derivatives **19**, **20** and **21** a clear differentiation in the absorption bands of the nucleobases (260–290 nm) and the coumarin dye (393 nm) can be made. The maximum absorption at 393 nm corresponds to the phenolate anion species (Figure 3A). The absorption and emission efficiencies are quantified on the basis of molar extinction coefficients (ε [$cm^{-1}\,M^{-1}$]; **19** = 15300, **20** = 20300, **21** = 24000). The N(3)-dye conjugate **19** has a lower extinction coefficient than **20**, whereas the bis-dye adduct **21** has a higher one.

A reversal in the signal intensities was observed in the fluorescence spectra of the dye conjugates (**19** > **20** > **21**), with the lowest fluorescence for the bis-adduct (Figure 3B). The fluorescence emission maxima for the dye conjugates are found to be identical, with a 476 nm emission when excited at 393 nm. Apparently, the fluorescence of bis-dye conjugate **21** was strongly quenched. This was supported by the determination of the quantum yield in distilled water with quinine sulfate as standard ($\Phi_f = 0.53$)[47] resulting in the following values: **19** ($\Phi_f = 0.65$), **20** ($\Phi_f = 0.32$) and **21** ($\Phi_f = 0.23$). From the number of dye residues one should expect the opposite behaviour. This quenching might be the result of proximal interaction of the coumarin labels.

The conjugate **19**, with a short linker and only one dye, showed higher fluorescence than the bis-adduct **21**. Here, any potential stacking interaction might not be possible due to the minimal length of the linker; in addition, an enlargement of the mesomeric system by electronic coupling between the dye and the nucleobase through the linker moiety could make a favourable contribution. These results led us to study the influ-

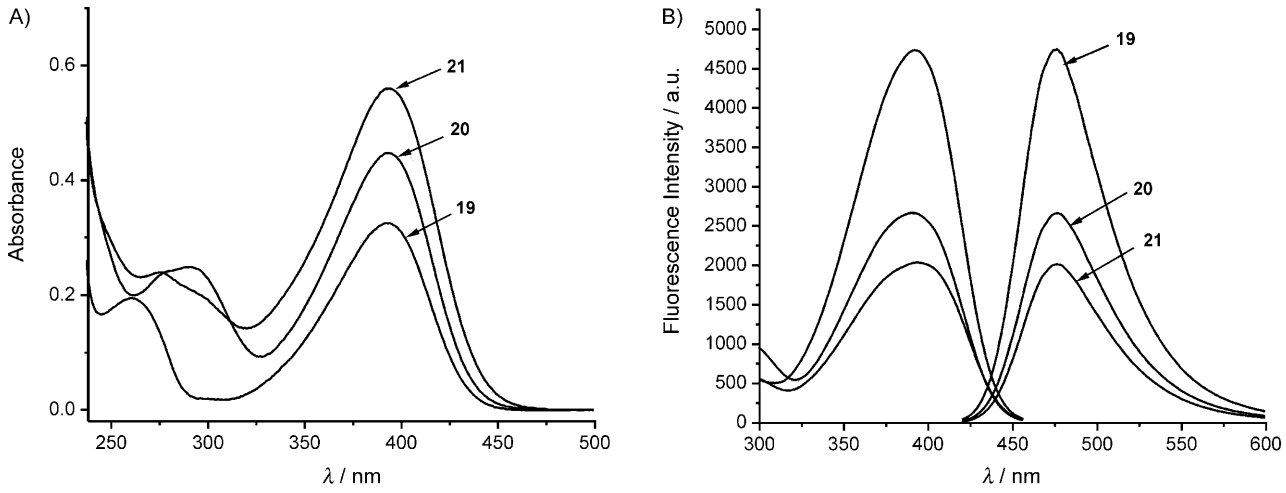

Figure 3. A) UV/Vis spectra of nucleoside dye conjugates **19**–**21**. B) Fluorescence excitation and emission spectra of **19**–**21** (2×10^{-5} M concentration) measured in Tris-HCl buffer (pH 8.5, 0.1 M).

ence of these nucleosides on the fluorescence properties of single-stranded and double-stranded DNA.

Dye functionalization of oligonucleotides by the azide–alkyne click reaction and fluorescence properties of the dye conjugates: The click reaction was performed between the single-stranded oligonucleotide 5′-d(TAG G**1a**C AAT ACT) (**14**), containing the dU analogue with two terminal triple bonds, and 3-azido-7-hydroxycoumarin (**4**). The reaction was performed in aqueous solution at room temperature in the presence of a 1:1 complex of $CuSO_4$·TBTA [tris(benzyltriazolylmethyl)amine] and TCEP [tris(carboxyethyl)phosphine] to furnish the strongly fluorescent functionalized oligonucleotide **22** (Scheme 5). The oligonucleotide 5′-d(TAG G**2**C AAT ACT) (**18**), containing N(3)-propargyl-2′-deoxyuridine (**2**) at the same position, was used in a similar way, and the click reaction was performed as described above to generate strongly fluorescent oligonucleotide conjugate **23**. The 5-substituted coumarin conjugate **24** has already been reported from our laboratory.[19] The formation of click products was confirmed by MALDI-TOF mass spectrometry as well as by enzymatic hydrolysis, which revealed the complete consumption of the starting oligonucleotides.

Next, the fluorescence properties of such oligonucleotides (**22**–**24**) containing different side chain dye moieties (**19**–**21**) located at the same position in the oligonucleotide sequence were studied. According to the data discussed above, the fluorescence of coumarin dye conjugates is expected to be pH-dependent. In order to demonstrate this, experiments were performed in buffer at pH 7.0 and 8.5. As illustrated in Figure 4, from pH 7.0 to 8.5 significant enhancements in the fluorescence emission were observed for all dye conjugates. The generation of a phenolate anion of coumarin dye causes the fluorescence to change. Fluorescence quenching of the two-dye conjugate **21** and a higher fluorescence for **19** were observed at pH 8.5 when they are present in ss-DNA (Figure 4). A similar result was observed for the free nucleoside dye conjugates. The excitation spectrum of the ss-DNA **22** containing bis-dye compound at pH 7.0 shows a broad peak around 350 nm, which corresponds to a mixed spectrum of the neutral and the anionic dye. From these results it can be concluded that for the second dye conjugate it is more difficult to generate a second anionic dye species when the first dye is already deprotonated. An alternative explanation for the altered excitation spectrum in **22** could be the formation of aggregates between the coumarin moieties.

Next, the fluorescence properties of duplex DNA were investigated at pH 8.5. In the case of oligonucleotide **23**, containing N(3)-dye conjugate **19**, the fluorescence was retained upon duplex formation at an emission wavelength of 479 nm (Figure 5A). This result was to be expected, because there is no formation of a base pair due to the blocked N(3)-position and the dye does not recognize the base pair if it is linked to a single chain or a double-stranded oligonucleotide. In contrast to this, the fluorescence of duplex containing two-dye residue **21** is significantly decreased relative to the single strand (Figure 5B), as has been reported for many other cases.

The fluorescence change upon hydrolysis of single-stranded DNA containing one dye conjugate was determined by snake venom phosphodiesterase/alkaline phosphatase digestion. The fluorescence emission was recorded at different time intervals. In the case of ss-DNA containing N(3)-dye nucleoside **19** (Figure 6A), an increase in the fluorescence emission was found after complete enzymatic digestion. The HPLC profile of the reaction products obtained after enzymatic digest shows the formation of a clean click digestion pattern (Figure 6B).

Click conjugation of oligonucleotides with AZT performed on solid support: Here we demonstrated Huisgen–Sharpless–Meldal cycloaddition on solid support with the CPG-bound oligonucleotide **25** (Scheme 6) and the antivirally active AZT (**3**). For this purpose the CPG-bound hexamer oligonucleotide 5′-d((5′-*O*-$(MeO)_2$Tr)GCA **1a**GC) was used as a starting material. The $(MeO)_2$Tr protecting group was preserved on the CPG-bound oligonucleotide, and the click reaction was performed as described above to form the crude click functionalized oligomer **26**. The excess starting materials and the reagents were re-

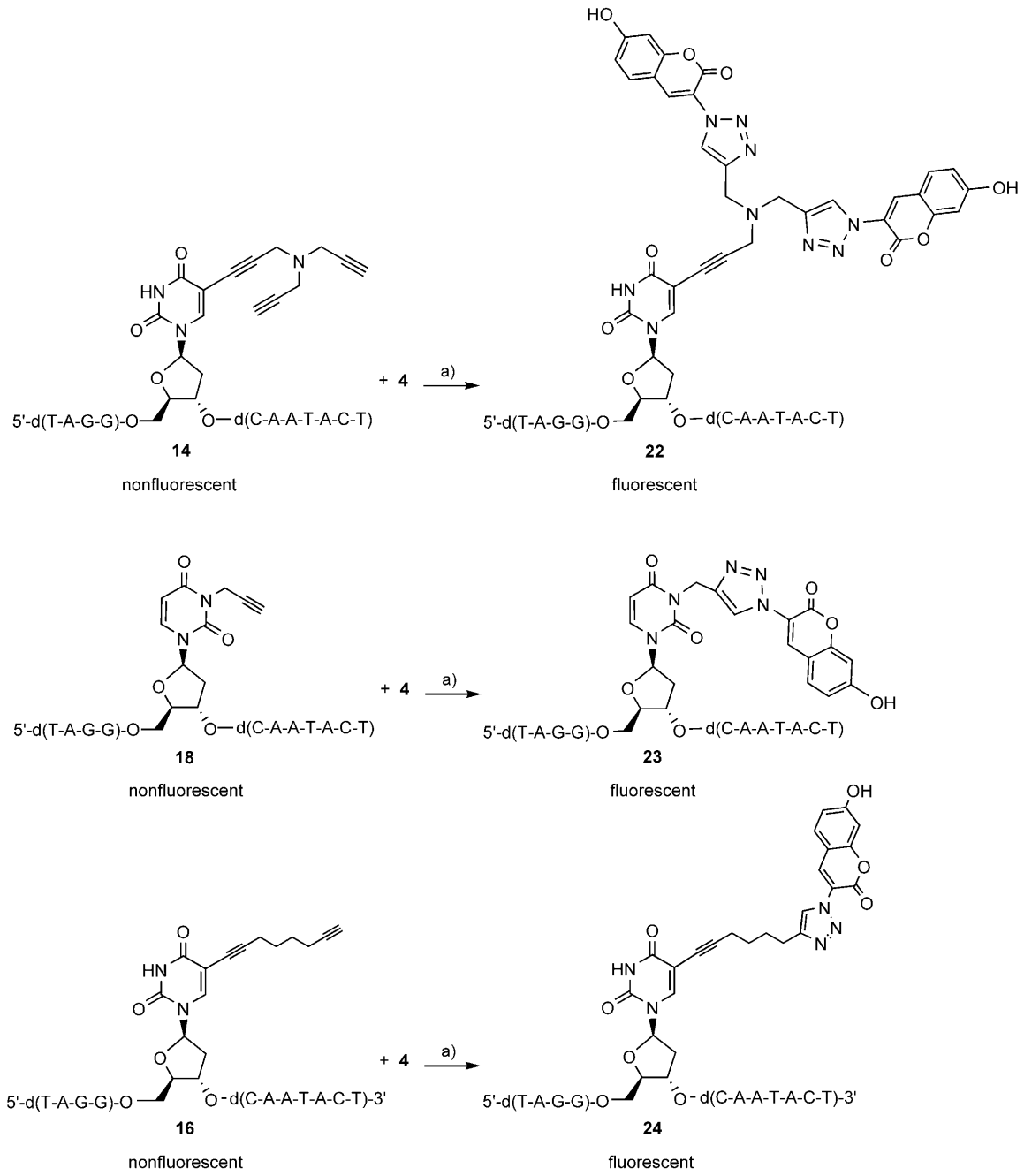

Scheme 5. Formation of oligonucleotide dye conjugates by click reactions. a) $CuSO_4$-TBTA, TCEP, H_2O/DMSO/*t*BuOH, RT.

moved by washing the crude matrix-bound **26** with MeOH/H_2O (1:1). Thereafter, the solid support was removed by standard deprotection conditions (25% aqueous ammonia solution, 60 °C for 14 h). During this procedure the protecting groups attached to the nucleobases were also removed. The 5′-*O*-dimethoxytrityl oligonucleotide was then further purified by reversed-phase HPLC (RP-18 column). The $(MeO)_2Tr$ group was then removed from the oligonucleotide, and further purification (see Experimental Section) yielded **27**. The structure of the ligated product was confirmed by MALDI-TOF-MS (Table S1) and by enzymatic hydrolysis (Figure 7). The click product moves more slowly than the starting nucleoside. The advantage of a click reaction on a solid support is that one can easily remove unwanted starting materials and reagents, which makes the purification easy, and clean click products were formed.

Conclusions

Double click reactions have been performed on nucleosides and oligonucleotides containing a 5-tripropargylamine side chain, bearing two terminal triple bonds, at the 5-position of 2′-deoxyuridine. For this, 5-tripropargylamine-2′-deoxyuridine (**1 a**) was prepared from the corresponding 5-iodo nucleoside

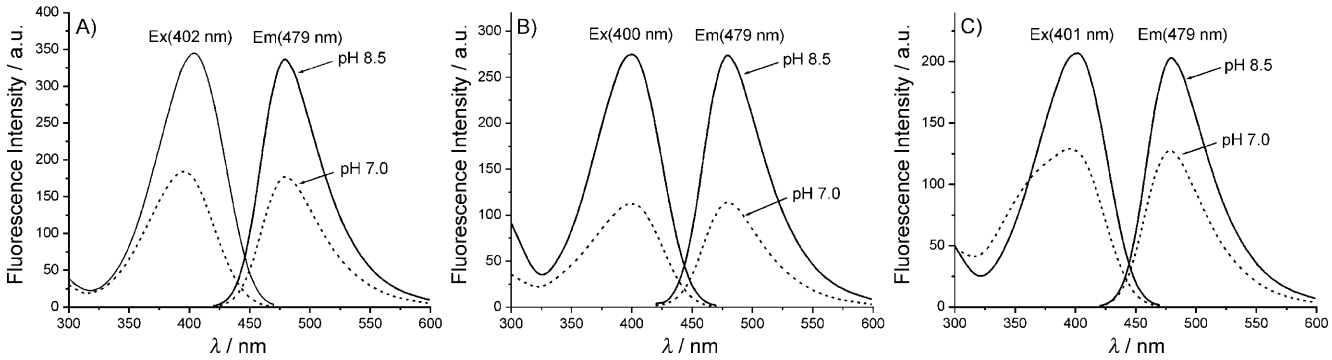

Figure 4. Fluorescence excitation and emission spectra of A) 1.0 μM single-stranded oligonucleotide **23**, B) **24**, and C) **22** measured at room temperature in buffer at pH 7.0 and pH 8.5.

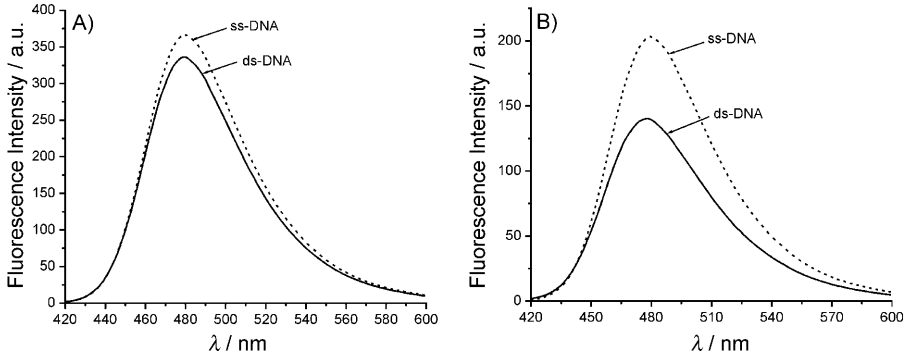

Figure 5. Fluorescence emission spectra A) of 1.0 μM single-strand **23** and duplex DNA **23·13** (1.0 μM of each strand), B) of **22** (1.0 μM single strand) and duplex DNA **22·13** in pH 8.5 buffer [NaCl (1 M), $MgCl_2$ (100 mM) and Na cacodylate (60 mM)].

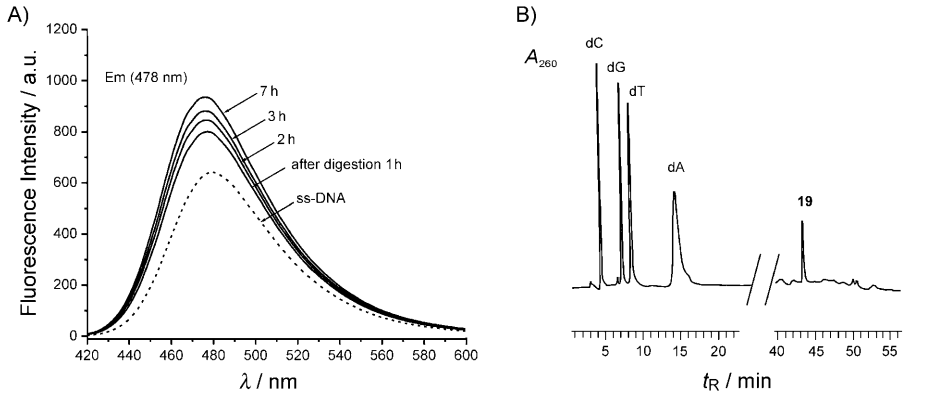

Figure 6. A) Fluorescence emission associated with the enzymatic digestion of single-stranded oligonucleotide 5′-d(TAG G**19**C AAT ACT) (**23**, 4 μM) with snake venom phosphodiesterase followed by alkaline phosphatase in Tris-HCl buffer (pH 8.5, 0.1 M). B) HPLC profile of the enzymatic hydrolysis products of **23** in Tris-HCl buffer (pH 8.5, 0.1 M) at 37 °C. Gradient: 20 min 100% A, 20–60 min 0–30% B in A, flow rate 0.7 mL min^{-1} [A = $(Et_3NH)OAc$ (pH 7.0, 0.1 M)/MeCN 95:5, B = MeCN].

and oligonucleotides were prepared by solid-phase synthesis. It was found that the sterically demanding 5-tripropargylamine residue (**1a**) is well accommodated in the DNA duplex and that the **1a**–dA base pair is as stable as the dT–dA pair. Such nucleosides and oligonucleotides containing tripropargylamine derivatives were further functionalized with the non-fluorescent azidocoumarin **4** by Huisgen–Sharpless–Meldal click chemistry to generate a set of highly fluorescent bis-coumarin conjugates. The conjugation of oligonucleotides containing branching elements with AZT (3′-azido-3′-deoxythymidine) on a solid support by click chemistry was also demonstrated. Of the various bioconjugates, the ss-DNA containing a rigid N(3)-1,2,3-triazolyl one-dye nucleoside **19** was found to be more fluorescent than those containing bis-dye adduct **21** or a dye conjugate **20** with a flexible linker. Apparently, the coumarin residues of the branched two-dye conjugate shows self-quenching.

Our branched oligonucleotides still form stable base pairs with the "clickable" moieties and tripropargylamine by the Pd-assisted Sonogashira cross-coupling reaction. For comparison, alkynyl residues with only one terminal triple bond in the 5-position (**1b**)[20] or at the N(3)-position of 2′-deoxyuridine (**2**) were also used. The nucleosides were converted into phosphoramidite building blocks, protruding into the major groove of duplex DNA. The advantage of this methodology is the difunctionalization of both terminal triple bonds in **1a**, which can be simultaneously employed in the click reaction. Even space-demanding residues are nicely accepted because the formation of triazole units

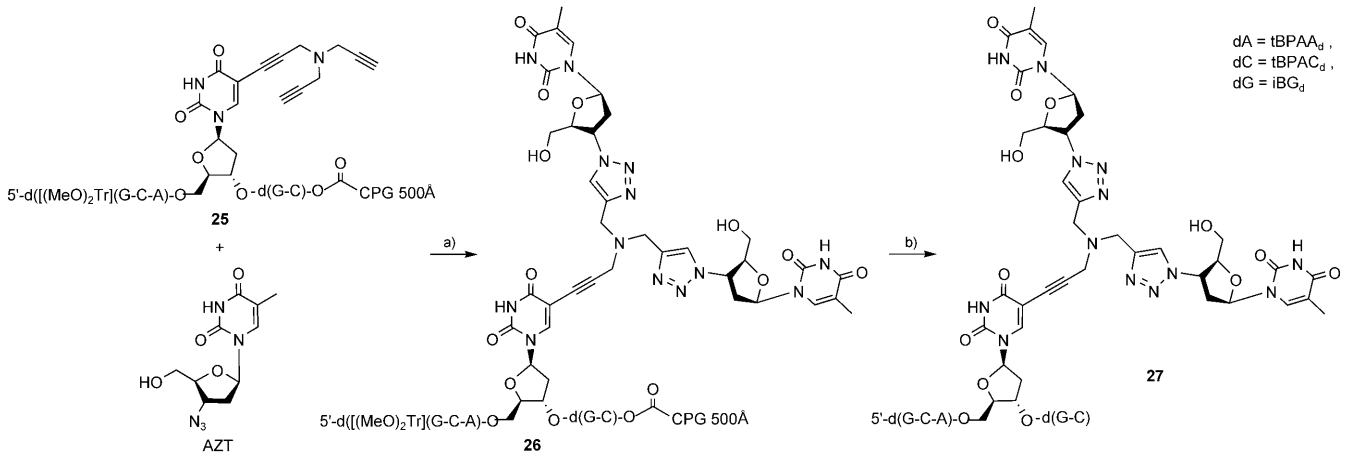

Scheme 6. Difunctionalization of a dialkynylated oligonucleotide with AZT on solid support. * The phosphates in solid-support-bound oligonucleotide **26** are *O*-cyanoethyl-protected. a) $CuSO_4$-TBTA, TCEP, H_2O/DMSO/*t*BuOH, RT; b) aq. NH_3, 60 °C, 14 h, 2% DCA/CH_2Cl_2.

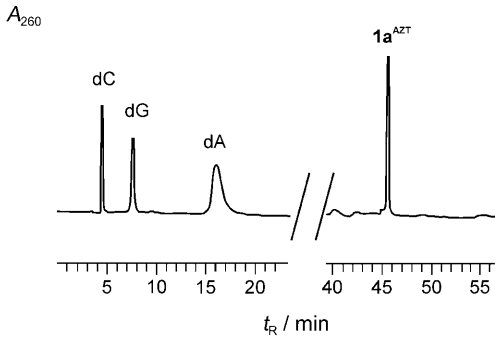

Figure 7. HPLC profile of the enzymatic hydrolysis products of oligonucleotide 5′-d(GC A**1 a**^{AZT}GC) **27** obtained by digestion with snake venom phosphodiesterase and alkaline phosphatase in Tris-HCl buffer (pH 8.5, 0.1 M) at 37 °C. Gradient: 20 min 100% A, 20–60 min 0–30% B in A, flow rate 0.7 mL min^{-1} [A = (Et_3NH)OAc (pH 7.0, 0.1 M)/MeCN 95:5, B = MeCN].

drives the reaction towards the difunctionalized conjugates, resulting from the excellent Cu(I) ligand-binding properties of tripropargylamine derivatives.[48] No more adducts were detected. Simultaneous incorporation of two reporter molecules is thus achieved (proteins, carbohydrates or lipids). Furthermore, dendrimeric side-chain units can be constructed from the branching unit by click conjugation with azido compounds carrying branched triply bonded side chains.[48] The water tolerance and the orthogonal character of this methodology allow it to be performed either on solid support or in solution.

Experimental Section

General: All chemicals were purchased from Acros, Aldrich, Sigma or Fluka (Sigma–Aldrich). Solvents were of laboratory grade. Thin-layer chromatography (TLC): aluminium sheets, silica gel 60 F_{254}, 0.2 mm layer (VWR International, Darmstadt, Germany). Column flash chromatography (FC): silica gel 60 (VWR International, Darmstadt, Germany) at 0.4 bar; Sample collection with an UltroRac II fractions collector (LKB Instruments, Sweden). UV spectra: U-3200 spectrometer (Hitachi, Tokyo, Japan); λ_{max} (ε) in nm. NMR Spectra: Avance 250 or Avance 300 spectrometers (Bruker, Karlsruhe, Germany), at 250.13 or 300.15 MHz for ^1H and ^{13}C; δ in ppm relative to Me_4Si as internal standard or external 85% H_3PO_4 for ^{31}P. *J* values in Hz. Elemental analyses were performed at the Mikroanalytisches Laboratorium Beller (Göttingen, Germany). Electron spray ionization (ESI) MS for the nucleosides: Bruker-Daltonics-MicroTOF spectrometer with loop injection (Bremen, Germany).

Fluorescence measurements: All measurements were performed in double-distilled water at room temperature. Absorption spectra were measured with a U-3200 UV/Vis spectrometer. In order to avoid inner filter effects the sample was not allowed to exceed 0.1 at the excitation wavelength in standard quartz cuvettes with a path length of 1 cm. Fluorescence spectra were recorded in the wavelength range between 320 and 600 nm with a Fluorescence Spectrophotometer F-2500 (Hitachi, Tokyo, Japan). For all calculations the water background was subtracted from the sample. The fluorescence quantum yields were determined with quinine sulfate in H_2SO_4 (0.1 N, fluorescence quantum yield 0.53)[42] as a standard through the following relationship [Eq. (1)]:

$$\Phi_{f.sample} = \Phi_{f.standard} \times (F_{sample}/F_{standard}) \times (A_{standard}/A_{sample}) \quad (1)$$

where $\Phi_{f.sample}$ is the unknown fluorescence quantum yield of the fluorophore, *F* is the integrated fluorescence intensity, and *A* is the absorbance in 1 cm cuvettes, never exceeding 0.1 at and above the excitation wavelength.

Synthesis, purification and characterization of the oligonucleotides: The oligonucleotide synthesis was performed on a DNA synthesizer, model ABI 392–08 (Applied Biosystems, Weiterstadt, Germany) at 1 μmol scale with the phosphoramidites **9** and **11** by the synthesis protocol for 3′-(2-cyanoethyl phosphoramidites) (user's manual for the 392 DNA synthesizer, Applied Biosystems, Weiterstadt, Germany). The coupling efficiency was always higher than 95%. After cleavage from the solid support with aqueous NH_3 solution (25%) for 14–16 h at 60 °C (during this process the amine protecting groups of the nucleobases [adenine, cytosine with *t*BPA (4-*tert*-butylphenoxy)acetyl protecting group and guanine with iB (isobutyryl)] were removed. The purification of 5′-dimethoxytrityl oligomers was carried out by reversed-phase HPLC (Merck–Hitachi-HPLC; RP-18 column; gradient system [A = (Et_3NH)OAc (pH 7.0, 0.1 M)/MeCN 95:5, B = MeCN]: 3 min 20% B in A, 12 min 20–50% B in A and 25 min 20% B in A; flow rate 1.0 mL min^{-1}. The purified

"trityl-on" oligonucleotides were treated with dichloroacetic acid in CH_2Cl_2 (2.5%) for 5 min at 0 °C to remove the 4,4′-dimethoxytrityl residues. The detritylated oligomers were purified again by reversed-phase HPLC (gradient: 0–20 min 0–20% B in A; flow rate 1 mL min^{-1}). The purification of click-functionalized oligonucleotides **22** and **23** was performed in trityl-off mode by reversed-phase HPLC (gradient: 0–25 min 0–30% B in A, flow rate 0.8 mL min^{-1}). The oligomers were desalted on a short column (RP-18, silica gel) and lyophilized on a Speed-Vac evaporator to yield colourless solids, which were frozen at −24 °C.

Melting curves were measured with a Cary 100 Bio UV/Vis spectrophotometer with a heating rate of 1 °C min^{-1}. The enzymatic hydrolysis of the oligonucleotides containing **1a** and **19** was performed with snake venom phosphodiesterase (EC 3.1.15.1, *Crotallus adamanteus*) and alkaline phosphatase (EC 3.1.3.1, *Escherichia coli* from Roche Diagnostics, GmbH, Germany) in Tris-HCl buffer (pH 8.5, 0.1 M) at 37 °C, and was analysed by reversed-phase HPLC (RP-18, at 260 nm) showing the peaks of the modified and unmodified nucleosides (Figure 1). Quantification of the constituents was made on the basis of the peak areas, which were divided by the extinction coefficients (ε_{260}) of the nucleosides: dA = 15400 (H_2O), dC = 7300 (H_2O), dG = 11700 (H_2O), dT = 8800 (H_2O), **1a** = 3700 (MeOH), **19** = 11000 (MeOH). The molecular masses of the oligonucleotides were determined by MALDI-TOF Biflex-III mass spectrometry (Bruker Saxonia, Leipzig, Germany) and with an Applied Biosystems Voyager DE PRO instrument with 3-hydroxypicolinic acid (3-HPA) as a matrix. The detected masses were identical with the calculated values (Table S1). The amount of DNA was calculated on the basis of the extinction coefficients of modified and unmodified monomers with use of an average hypochromicity of 20%.

1-(2-Deoxy-β-D-*erythro*-pentofuranosyl)-5-{3-[di(prop-2-ynyl)amino]prop-1-ynyl}uracil (1a): [$Pd(PPh_3)_4$] (163 mg, 0.14 mmol), anhydrous Et_3N (344 mg, 3.4 mmol) and tri(prop-2-ynyl)amine (1.8 g, 13.7 mmol) were added successively to a suspension of 5-iodo-2′-deoxyuridine (**5**, 500 mg, 1.41 mmol) and CuI (54 mg, 0.28 mmol) in anhydrous DMF (7 mL). The mixture was stirred at room temperature under argon, and the reaction was allowed to proceed until the starting material had been consumed (TLC monitoring). The reaction mixture was concentrated, and the residue was purified by FC (silica gel, column 15×3 cm, CH_2Cl_2/MeOH 94:6) to give the product **1a** (350 mg, 69%) as a colourless, amorphous solid. TLC (CH_2Cl_2/MeOH 9:1): R_f = 0.62. ^{1}H NMR ([D_6]DMSO): δ = 2.1 (m, 2H; H-2′), 3.23 (s, 2H; 2 × C≡CH), 3.40 (s, 4H; 2 × CH_2), 3.56 (s, 2H; CH_2), 3.63 (m, 2H; H-5′), 3.78 (m, 1H; H-4′), 4.22 (m, 1H; H-3′), 5.11 (t, J = 5.0 Hz, 1H; 5′-OH), 5.25 (d, J = 4.2 Hz, 1H; 3′-OH), 6.10 (t, J = 6.4 Hz, 1H; H-1′), 8.2 (s, 1H; H-6), 11.63 ppm (s, 1H; N3-H); UV (MeOH): λ_{max} (ε) = 230 (12100), 291 nm (12800 mol^{-1} dm^3 cm^{-1}); elemental analysis calcd (%) for $C_{18}H_{19}N_3O_5$ (357.13): C 60.50, H 5.36, N 11.76; found: C 60.64, H 5.45, N 11.65.

1-(2-Deoxy-β-D-*erythro*-pentofuranosyl)-3-(prop-2-yn-1-yl)uracil (2): A solution of propargyl bromide (0.65 mL, 5.84 mmol) was added to a solution of 2′-deoxyuridine (**7**, 1.0 g, 4.38 mmol) and potassium carbonate (1.66 g, 12.0 mmol) in DMF/acetone (1:1, *v/v*, 22 mL), and the system was stirred at 50 °C for 3 days. The reaction mixture was filtered and evaporated to dryness. Distilled water (40 mL) was added to the residue, and the solution was extracted with CH_2Cl_2 (50 mL). The organic layer was washed with saturated NaCl (50 mL), dried over Na_2SO_4 and then concentrated. Purification by FC (silica gel, column 15×3 cm, CH_2Cl_2/MeOH 9:1) gave **2** (840 mg, 72%) as a colourless foam. TLC (CH_2Cl_2/MeOH 9:1): R_f = 0.43. ^{1}H NMR ([D_6] DMSO): δ = 2.04–2.20 (m, 2H; H-2′), 3.11 (s, 1H; C≡CH), 3.56 (m, 2H; H-5′), 3.80 (m, 1H; H-4′), 4.23 (m, 1H; H-3′), 4.50 (s, 2H; CH_2N), 5.05 (m, 1H; 5′-OH), 5.29 (d, J = 3.1 Hz, 1H; 3′-OH), 5.83 (d, J = 8.1 Hz, 1H; H-5), 6.18 (t, J = 6.6 Hz, 1H; H-1′), 7.97 ppm (d, J = 8.1 Hz, 1H; H-6); UV (MeOH): λ_{max} (ε) = 263 nm (8800 mol^{-1} dm^3 cm^{-1}); elemental analysis calcd (%) for $C_{12}H_{14}N_2O_5$ (266.09): C 54.13, H 5.30, N 10.52; found: C 54.20, H 5.26, N 10.48.

3-(2-Deoxy-β-D-*erythro*-pentofuranosyl)-6-{3-[di(prop-2-ynyl)amino]methyl}-3*H*-furo[2,3-*d*]pyrimidin-2-one (6): CuI (50 mg, 0.26 mmol) was added to a solution of compound **1a** (250 mg, 0.70 mmol) in Et_3N/MeOH (3:7, *v/v*, 30 mL), and the mixture was heated at reflux for 12 h. The solvent was evaporated in vacuo, and the crude product was purified by FC (silica gel, column 15× 3 cm, CH_2Cl_2/MeOH 93:7) to give **6** (200 mg, 80%) as a colourless, amorphous solid; TLC (CH_2Cl_2/MeOH 9:1): R_f = 0.55. ^{1}H NMR ([D_6]-(DMSO): δ = 2.05 (m, 1H; H_α-2′), 2.40 (m, 1H; H_β-2′), 3.25 (s, 2H; 2 × C≡CH), 3.41 (s, 4H; 2 × CH_2), 3.62 (m, 2H; H-5′), 3.68 (s, 2H; CH_2), 3.92 (m, 1H; H-4′), 4.22 (m, 1H; H-3′), 5.12 (t, J = 5.20 Hz, 1H; 5′-OH), 5.28 (d, J = 4.28 Hz, 1H; 3′-OH), 6.16 (t, J = 6.10 Hz, 1H; H-1′), 6.64 (s, 1H; H-5); 8.76 ppm (s, 1H; H-4); UV (MeOH): λ_{max} (ε) = 244 (12400), 329 nm (6400 mol^{-1} dm^3 cm^{-1}); elemental analysis calcd (%) for $C_{18}H_{19}N_3O_5$ (357.13): C 60.50, H 5.36, N 11.76; found: C 60.39, H 5.44, N 11.66.

1-[5-*O*-(4,4′-Dimethoxytrityl)-2-deoxy-β-D-*erythro*-pentofuranosyl]-5-{3-[di(prop-2-ynyl)amino]prop-1-ynyl}-uracil (8): Compound **1a** (240 mg, 0.67 mmol) was dried by repeated co-evaporation with anhydrous pyridine (2×5 mL) before dissolution in anhydrous pyridine (8 mL). 4,4′-Dimethoxytrityl chloride (300 mg, 0.88 mmol) was then added to the remaining solution in three portions at room temperature with stirring for 6 h. MeOH (2 mL) was then added, and the mixture was stirred for another 30 min. The reaction mixture was dissolved in CH_2Cl_2 (2×50 mL) and extracted with aqueous $NaHCO_3$ solution (5%, 100 mL) followed by H_2O (80 mL), dried over Na_2SO_4 and then concentrated. Purification by FC (silica gel, column 15×3 cm, CH_2Cl_2/acetone 1:1) gave **8** (340 mg, 77%) as a colourless foam. TLC (CH_2Cl_2/MeOH 94:6): R_f = 0.52. ^{1}H NMR ([D_6] DMSO): δ = 2.2 (m, 2H; H-2′), 3.22 (s, 2H; 2 × C≡CH), 3.30–3.40 (8H; H-5′, 2 × CH_2, CH_2), 3.73 (s, 6H; 2 × OCH_3), 3.91 (m, 1H; H-4′), 4.27 (m, 1H; H-3′), 5.34 (d, J = 3.7 Hz, 1H; 3′-OH), 6.10 (t, J = 6.2 Hz, 1H; H-1′), 6.86–7.41 (m, 13H; H-arom), 7.92 (s, 1H; H-6), 11.68 ppm (s, 1H; N3-H); UV (MeOH): λ_{max} (ε) = 233 (32000), 284 nm (12400 mol^{-1} dm^3 cm^{-1}); elemental analysis calcd (%) for $C_{39}H_{37}N_3O_7$ (659.26): C 71.00, H 5.65, N 6.37; found: C 70.94, H 5.75, N 6.40.

1-[5-*O*-(4,4′-Dimethoxytrityl)-2-deoxy-β-D-*erythro*-pentofuranosyl]-5-{3-[di(prop-2-yny)amino]prop-1-ynyl}-uracil 3′-(2-cyanoethyl)-*N*,*N*-diisopropylphosphoramidite (9): A stirred solution of **8** (170 mg, 0.26 mmol) in anhydrous CH_2Cl_2 (3 mL) was pre-flushed with argon and treated with (iPr)$_2$EtN (85 μL, 0.51 mmol), followed by 2-cyanoethyl-*N*,*N*-diisopropylphosphoramidochloridite (107 μL, 0.46 mmol). After stirring for 1 h at room temperature, the solution was diluted with CH_2Cl_2 (30 mL) and extracted with aqueous $NaHCO_3$ solution (5%, 20 mL). The organic layer was dried over Na_2SO_4 and concentrated. FC (silica gel, column 10×2 cm, CH_2Cl_2/acetone 80:20) gave **9** (140 mg, 63%) as a colourless foam. TLC (CH_2Cl_2/acetone 95:5): R_f = 0.67. ^{31}P NMR ($CDCl_3$): 150.25, 149.6 ppm; elemental analysis calcd (%) for $C_{48}H_{54}N_5O_8P$ (859.37): C 67.04, H 6.33, N 8.14; found: C 66.88, H 6.45, N 8.25.

1-[5-*O*-(4,4′-Dimethoxytrityl)-2-deoxy-β-D-*erythro*-pentofuranosyl]-3-(prop-2-yn-1-yl)uracil (10): Compound **2** (560 mg, 2.10 mmol) was dried by repeated co-evaporation with anhydrous pyridine (2×5 mL) before dissolving in anhydrous pyridine (10 mL). 4,4′-Dimethoxytrityl chloride (900 mg, 2.66 mmol) was then added in three portions to the remaining solution at room temperature

with stirring for 5 h. MeOH (2 mL) was then added, and the reaction mixture was dissolved in CH_2Cl_2 (2×50 mL) and extracted with aqueous $NaHCO_3$ solution (5%, 100 mL) followed by H_2O (80 mL), dried over Na_2SO_4, and then concentrated. Purification by FC (silica gel, column 15×3 cm, CH_2Cl_2/acetone 94:6) gave **10** (1.06 g, 89%) as a colourless foam. TLC (CH_2Cl_2/acetone 95:5): R_f=0.68. ^{1}H NMR ([D_6] DMSO): δ=2.20–2.25 (m, 2H; H-2′), 3.13 (s, 1H; C≡CH), 3.16–3.34 (m, 2H; H-5′), 3.73 (s, 6H; 2×OCH_3), 3.89 (m, 1H; H-4′), 4.30 (m, 1H; H-3′), 4.50 (s, 2H; CH_2N), 5.37 (d, J=4.3 Hz, 1H; 3′-OH), 5.52 (d, J=8.1 Hz, 1H; H-5), 6.18 (t, J=6.2 Hz, 1H; H-1′), 6.87–7.39 (m, 13H; H-arom), 7.72 ppm (d, J=8.0 Hz, 1H; H-6); UV (MeOH): λ_{max} (ε)=265 (11000), 234 nm (22000); elemental analysis calcd (%) for $C_{33}H_{32}N_2O_7$ (568.22): C 69.70, H 5.67, N 4.93; found: C 69.61, H 5.70, N 4.85.

1-[5-*O*-(4,4′-Dimethoxytrityl)-2-deoxy-β-D-*erythro*-pentofuranosyl]- 3-(prop-2-yn-1-yl)uracil 3′-(2-cyanoethyl)-*N*,*N*-diisopropylphosphoramidite (11): A stirred solution of **10** (500 mg, 0.88 mmol) in anhydrous CH_2Cl_2 (8 mL) was pre-flushed with argon and treated with (iPr)$_2$EtN (200 μL, 1.2 mmol), followed by 2-cyanoethyl-*N*,*N*-diisopropylphosphoramidochloridite (0.86 mmol, 200 μL). After stirring for 45 min at room temperature, the solution was diluted with CH_2Cl_2 (30 mL) and extracted with aqueous $NaHCO_3$ solution (5%, 20 mL). The organic layer was dried over Na_2SO_4 and concentrated. FC (silica gel, column 10×2 cm, CH_2Cl_2/acetone 9:1) gave **11** (400 mg, 59%) as a colourless foam. TLC (CH_2Cl_2/acetone 9:1): R_f=0.77. ^{31}P NMR ($CDCl_3$): 150.39, 149.92 ppm.

Preparation of click nucleoside 19 from 2 by Cu^I-catalysed cycloaddition: Sodium ascorbate (freshly prepared 1 M solution in water, 570 μL, 0.56 mmol) was added to a solution of compound **2** (100 mg, 0.37 mmol) and 3-azido-7-hydroxycoumarin (**4**, 87 mg, 0.43 mmol) in THF/H_2O/tBuOH (3:1:1, *v/v*, 4 mL), followed by the addition of copper(II) sulfate pentahydrate (7.5% in water, 465 μL, 0.139 mmol). The emulsion was stirred for 18 h at room temperature, concentrated and subjected to FC (silica gel, column 10×3 cm, CH_2Cl_2/MeOH 9:1). From the main zone, compound **19** (140 mg, 80%) was isolated as a yellowish solid. TLC (CH_2Cl_2/MeOH 9:1): R_f=0.32. ^{1}H NMR ([D_6] DMSO): δ=2.07–2.14 (m, 2H; H-2′), 3.56 (m, 2H; H-5′), 3.79 (m, 1H; H-4′), 4.23 (m, 1H; H-3′), 5.06–5.28 (m, 4H; 5′-OH, CH_2, 3′-OH), 5.82 (d, J=8.1 Hz, 1H; H-5), 6.20 (t, J=6.6 Hz, 1H; H-1′), 6.84–6.91 (m, 2H; H-arom), 7.74 (d, J=8.6, 1H; H-arom), 7.98 (d, J=8.1 Hz, 1H; H-6), 8.40 (s, 1H; C=CH), 8.55 (s, 1H; H-arom), 10.89 ppm (s, 1H; OH); UV (MeOH): λ_{max} (ε)=257 (11000), 346 nm (17400); HRMS-MALDI: *m/z*: 492.16 [*M*+Na]$^+$; $C_{21}H_{19}N_5O_8Na^+$ calcd 492.11.

Preparation of difunctionalized nucleoside 21 from 1a by Cu^I-catalysed cycloaddition: 2,6-Lutidine (33 μL, 0.283 mmol) was added to a mixture of compound **1a** (100 mg, 0.28 mmol) and 3-azido-7-hydroxycoumarin (**4**, 140 mg, 0.69 mmol) in acetonitrile (2 mL), followed by the addition of $Cu(MeCN)_4PF_6$ (5.3 mg, 0.014 mmol). The reaction mixture was stirred for 20 h at room temperature, concentrated and subjected to FC (silica gel, column 10×3 cm, CH_2Cl_2/MeOH 9:1). From the main zone, compound **21** (128 mg, 60%) was isolated as a yellowish solid. TLC (CH_2Cl_2/MeOH 9:1): R_f=0.28. ^{1}H NMR ([D_6] DMSO): δ=2.13–2.17 (m, 2H; H-2′), 3.50–3.61 (4H; H-5′, CH_2), 3.78 (m, 1H; H-4′), 3.93 (s, 4H; 2×CH_2), 4.24 (m, 1H, H-3′), 5.14 (1H; 5′-OH), 5.26 (1H; 3′-OH), 6.10 (t, J=6.5 Hz, 1H; H-1′), 6.88–6.91 (dd, J=8.6 Hz, 4H; H-arom), 7.71–7.74 (d, J=8.5 Hz, 2H; H-arom), 8.28 (s, 1H; H-6), 8.49 (s, 1H; C=CH), 8.58 (s, 1H; H-arom), 10.81 (s, 2H; OH), 11.63 ppm (s, N(3)-H); UV (MeOH): λ_{max} (ε)=291 (9200), 346 nm (22000 mol^{-1} dm^3 cm^{-1}); HRMS-MALDI: *m/z*: 786.18 [*M*+Na]$^+$; calcd for $C_{36}H_{29}N_9O_{11}Na^+$ 786.19.

Huisgen–Sharpless–Meldal [3+2] cycloaddition performed in aqueous solution with oligonucleotide 14 and nonfluorescent coumarin azide 4: $CuSO_4$·TBTA ligand complex (50 μL of a 20 mM stock solution in tBuOH/H_2O 1:9), tris-(carboxyethyl)phosphine (TCEP, 50 μL of a 20 mM stock solution in water), $NaHCO_3$ (20 mM, 30 μL), 3-azido-7-hydroxycoumarin (**4**, 70 μL of a 20 mM stock solution in THF) and DMSO (50 μL) were added to the single-stranded oligonucleotide **14** (39 nmol), and the reaction was run at room temperature for 30 h. The click product **22** was further purified by reversed-phase HPLC in trityl-off mode. The isolated yield of the click product **22** was greater than 55%. The molecular masses of the oligonucleotides were determined by MALDI-TOF spectra (Table S1).

Huisgen–Sharpless–Meldal [3+2] cycloaddition performed in aqueous solution with oligonucleotide 18 and nonfluorescent coumarin azide 4: $CuSO_4$·TBTA ligand complex (30 μL of a 20 mM stock solution in tBuOH/H_2O 1:9), tris-(carboxyethyl)phosphine (TCEP, 30 μL of a 20 mM stock solution in water), $NaHCO_3$ (20 mM, 20 μL), 3-azido-7-hydroxycoumarin (**4**, 50 μL of a 20 mM stock solution in THF) and DMSO (30 μL) were added to the single-stranded oligonucleotide **18** (38 nmol), and the reaction was run at room temperature for 30 h. The click product **23** was further purified by reversed-phase HPLC in trityl-off mode. The isolated yield of the click product **23** was greater than 55%. The molecular masses of the oligonucleotides were determined by MALDI-TOF spectra (Table S1).

Huisgen–Sharpless–Meldal [3+2] cycloaddition with 25 and AZT (3) performed on solid support: The single-stranded oligonucleotide **25** attached to a solid support (30 mg, 36 μmol g^{-1} loading 500 Å) bearing the $(MeO)_2$Tr-protected residue as well as the nucleobases adenine and cytosine with tBPA (4-*tert*-butylphenoxy)acetyl protection and guanine with isobutyryl (iB) protecting groups was suspended in an aqueous solution of H_2O/DMSO/tBuOH (3:1:1, *v/v*, 70 μL). To this were added $CuSO_4$·TBTA ligand complex (40 μL of a 20 mM stock solution in tBuOH/H_2O 1:9), tris-(carboxyethyl)phosphine (TCEP; 40 μL of a 20 mM stock solution in H_2O), $NaHCO_3$ (30 μL, 20 mM), AZT (**3**; 60 μL of a 20 mM stock solution in dioxane/H_2O 1:1), DMSO (40 μL), and the reaction mixture was stirred at room temperature for 24 h and then concentrated. The crude modified CPG-bound **26** was washed with H_2O/MeOH (1:1, *v/v*, 4 mL), followed by treatment with aqueous NH_3 solution (25%) for 14 h at 60 °C. During this procedure the oligonucleotide attached to the solid support as well as the protecting groups of the nucleobases were removed. The "trityl-on" oligonucleotide was purified by reversed-phase HPLC (see above). The detritylated oligonucleotide was further purified by reversed-phase HPLC to give **27**. For MALDI-TOF see Table S1.

Acknowledgements

We thank S. Budow and P. Leonard for measuring the NMR spectra. We also thank Dr. T. Koch from Roche Diagnostics, GmbH, Penzberg, Germany for the measurement of the MALDI spectra and Nhat Quang Tran for the oligonucleotide syntheses. Financial support by Roche Diagnostics, GmbH and ChemBiotech, Muenster, Germany is gratefully acknowledged.

Keywords: branched DNA · click chemistry · fluorescence · nucleosides · oligonucleotides

[1] R. Huisgen, *Angew. Chem.* **1963**, *75*, 604–637; *Angew. Chem. Int. Ed. Engl.* **1963**, *2*, 565–598.
[2] R. Huisgen, *1,3-Dipolar Cycloaddition Chemistry, Vol. 1* (Ed.: A. Padwa), Wiley, New York, **1984**, pp. 1–176.
[3] H. C. Kolb, M. G. Finn, K. B. Sharpless, *Angew. Chem.* **2001**, *113*, 2056–2075; *Angew. Chem. Int. Ed.* **2001**, *40*, 2004–2021.
[4] V. V. Rostovtsev, L. G. Green, V. V. Fokin, K. B. Sharpless, *Angew. Chem.* **2002**, *114*, 2708–2711; *Angew. Chem. Int. Ed.* **2002**, *41*, 2596–2599.
[5] C. W. Tornøe, C. Christensen, M. Meldal, *J. Org. Chem.* **2002**, *67*, 3057–3064.
[6] M. Sawa, T. S. Hsu, T. Itoh, M. Sugiyama, S. R. Hanson, P. K. Vogt, C. H. Wong, *Proc. Natl. Acad. Sci. USA* **2006**, *103*, 12371–12376.
[7] Q. Wang, T. R. Chan, R. Hilgraf, V. V. Fokin, K. B. Sharpless, M. G. Finn, *J. Am. Chem. Soc.* **2003**, *125*, 3192–3193.
[8] K. E. Beatty, F. Xie, Q. Wang, D. A. Tirrell, *J. Am. Chem. Soc.* **2005**, *127*, 14150–14151.
[9] a) J. Lietard, A. Meyer, J. J. Vasseur, F. Morvan, *J. Org. Chem.* **2008**, *73*, 191–200; b) P. M. E. Gramlich, S. Warncke, J. Gierlich, T. Carell, *Angew. Chem.* **2008**, *120*, 3491–3493; *Angew. Chem. Int. Ed.* **2008**, *47*, 3442–3444.
[10] T. S. Seo, Z. Li, H. Ruparel, J. Ju, *J. Org. Chem.* **2003**, *68*, 609–612.
[11] R. L. Weller, S. R. Rajski, *Org. Lett.* **2005**, *7*, 2141–2144.
[12] J. Gierlich, G. A. Burley, P. M. E. Gramlich, D. M. Hammond, T. Carell, *Org. Lett.* **2006**, *8*, 3639–3642.
[13] I. Géci, V. V. Filichev, E. B. Pedersen, *Chem. Eur. J.* **2007**, *13*, 6379–6386.
[14] P. Kočalka, N. K. Andersen, F. Jensen, P. Nielsen, *ChemBioChem* **2007**, *8*, 2106–2116.
[15] F. Seela, V. R. Sirivolu, *Helv. Chim. Acta* **2007**, *90*, 535–552.
[16] N. K. Devaraj, G. P. Miller, W. Ebina, B. Kakaradov, J. P. Collman, E. T. Kool, C. E. D. Chidsey, *J. Am. Chem. Soc.* **2005**, *127*, 8600–8601.
[17] T. S. Seo, X. Bai, H. Ruparel, Z. Li, N. J. Turro, J. Ju, *Proc. Natl. Acad. Sci. USA* **2004**, *101*, 5488–5493.
[18] F. Seela, V. R. Sirivolu, *Chem. Biodiversity* **2006**, *3*, 509–514.
[19] F. Seela, V. R. Sirivolu, P. Chittepu, *Bioconjugate Chem.* **2008**, *19*, 211–224.
[20] F. Seela, V. R. Sirivolu, *Org. Biomol. Chem.* **2008**, *6*, 1674–1687.
[21] T. Horn, C. A. Chang, M. S. Urdea, *Nucleic Acids Res.* **1997**, *25*, 4842–4849.
[22] F. Seela, S. Budow, P. Leonard, *Org. Biomol. Chem.* **2007**, *5*, 1858–1872.
[23] R. H. E. Hudson, A. H. Uddin, M. J. Damha, *J. Am. Chem. Soc.* **1995**, *117*, 12470–12477.
[24] N. Balgobin, A. Földesi, G. Remaud, J. Chattopadhyaya, *Tetrahedron* **1988**, *44*, 6929–6939.
[25] P. Agback, C. Glemarec, C. Sund, J. Chattopadhyaya, *Tetrahedron* **1992**, *48*, 6537–6554.
[26] H. Rosemeyer, E. Feiling, W. Nierling, F. Seela, *Nucleosides Nucleotides* **1999**, *18*, 1563–1564.
[27] M. S. Shchepinov, I. A. Udalova, A. J. Bridgman, E. M. Southern, *Nucleic Acids Res.* **1997**, *25*, 4447–4454.
[28] T. Horn, M. S. Urdea, *Nucleic Acids Res.* **1989**, *17*, 6959–6967.
[29] F. Seela, M. Zulauf, *Helv. Chim. Acta* **1999**, *82*, 1878–1898.
[30] M. J. Robins, P. J. Barr, *J. Org. Chem.* **1983**, *48*, 1854–1862.
[31] P. Acharya, P. Cheruku, S. Chatterjee, S. Acharya, J. Chattopadhyaya, *J. Am. Chem. Soc.* **2004**, *126*, 2862–2869.
[32] J. Graton, F. Besseau, M. Berthelot, E. D. Raczyńska, C. Laurence, *Can. J. Chem.* **2002**, *80*, 1375–1385.
[33] J. A. Brazier, T. Shibata, J. Townsley, B. F. Taylor, E. Frary, N. H. Williams, D. M. Williams, *Nucleic Acids Res.* **2005**, *33*, 1362–1371.
[34] G. Becher, J. He, F. Seela, *Helv. Chim. Acta* **2001**, *84*, 1048–1065.
[35] F. Seela, M. Zulauf, *Chem. Eur. J.* **1998**, *4*, 1781–1790.
[36] N. Ramzaeva, F. Seela, *Helv. Chim. Acta* **1996**, *79*, 1549–1558.
[37] F. Seela, M. Zulauf, *Synthesis* **1996**, 726–730.
[38] J. He, F. Seela, *Nucleic Acids Res.* **2002**, *30*, 5485–5496.
[39] T. W. Barnes III, D. H. Turner, *J. Am. Chem. Soc.* **2001**, *123*, 4107–4118.
[40] T. Kottysch, C. Ahlborn, F. Brotzel, C. Richert, *Chem. Eur. J.* **2004**, *10*, 4017–4028.
[41] F. Seela, K. I. Shaikh, *Tetrahedron* **2005**, *61*, 2675–2681.
[42] T. R. Chan, R. Hilgraf, K. B. Sharpless, V. V. Fokin, *Org. Lett.* **2004**, *6*, 2853–2855.
[43] R. S. Coleman, M. A. Berg, C. J. Murphy, *Tetrahedron* **2007**, *63*, 3450–3456.
[44] C. A. M. Seidel, A. Schulz, M. H. M. Sauer, *J. Phys. Chem.* **1996**, *100*, 5541–5553.
[45] D. W. Fink, W. R. Koehler, *Anal. Chem.* **1970**, *42*, 990–993.
[46] K. Sivakumar, F. Xie, B. M. Cash, S. Long, H. N. Barnhill, Q. Wang, *Org. Lett.* **2004**, *6*, 4603–4606.
[47] A. N. Fletcher, *Photochem. Photobiol.* **1969**, *9*, 439–444.
[48] J. W. Lee, B.-K. Kim, *Bull. Korean Chem. Soc.* **2005**, *26*, 658–660.

Received: May 7, 2008
Published online on September 9, 2008

